Journal of Statistical Physics, Vol. 43, Nos. 5/6, 1986

Simulations: A Tool for Studying Quantum Condensed Matter Systems[1]

D. J. Scalapino[2]

Quantum Monte Carlo techniques provide a new method for studying the properties of condensed matter systems. A review of this approach and the type of information which it can provide is given.

KEY WORDS: Quantum Monte Carlo; condensed matter; quantum lattice gas; *XXZ*.

1. INTRODUCTION

Over the years the Monte Carlo technique described in the pioneering work of Metropolis et al.[1] has been widely used for a rich variety of problems in classical physics More recently, this technique,[2-4] along with other stochastic methods[5] has become an important new tool in the study of quantum condensed matter systems. Here I will review the structure of these simulations using as an example an interacting spinless fermion model. However, before getting into details, it is useful to consider what types of questions simulations can help us explore. The following represents a short list of models which have been or are currently being studied using quantum Monte Carlo techniques.

(1) Do 1-D metallic chains with polarizable side groups exhibit high temperature superconducting pair fluctuations[6] as originally suggested by Little?[7] If they do, then what regions of the parameter space (one-electron overlap, Coulomb integrals, exciton frequency, band filling, etc.) are most favorable? If there is no pairing, what type of

[1] Talk presented at the Frontiers of Monte Carlo Meeting, Los Alamos National Laboratory, September, 1985.

[2] Department of Physics, University of California, Santa Barbara, California 93106.

0022-4715/86/0600-0757$05.00/0 © 1986 Plenum Publishing Corporation

correlations (e.g., charge density wave, spin density wave) are present? What happens in two dimensions?

(2) A variety of adsorbed gas problems have been mapped onto 2-D Ising, or more generally, q state Potts models. What happens if the system consists of light atoms so that their quantum mechanical translational motion is important?[9] $CoCl_2$ has been intercollated into graphite and forms a 2-D quantum XXZ model. What are its phase properties?[10]

(3) Can a nondegenerate Hubbard model with a repulsive U have a ferromagnetic phase or does it only exhibit antiferromagnetism? Under what conditions does it exhibit these phases?[11] Can it have a triplet superconducting phase? What are the properties of a degenerate Hubbard model?[12]

(4) How does a quasi-1-D material, in which the coupling along one axis are much stronger than along the other axes, such as KCP or TTF–TCNQ, order as the temperature is lowered?[13] What is the nature of the metal insulating transition? What effect do the various interaction strengths, the band fillings, or impurities have on the transition? These are just a few of the questions one might consider. Here at Los Alamos one should certainly add: Does a periodic Anderson or Kondo lattice model exhibit a tendency toward triplet pairing or anisotropic s-wave pairing?

There are clearly a wide variety of questions which could be asked, and I've selected these because I'm familiar with them. Nevertheless, they give a flavor of the type of correlations which are being explored with simulations. The goals of these simulations vary. On the most basic level one would like to know whether a given model contains the essential physical phenomena. Does Little's model have large superconducting fluctuations? Can a nondegenerate Hubbard model have a ferromagnetic phase or a triplet pairing phase? How does the order onset in quasi-1-D systems? If the *phenomena* is there, we may want to proceed to develop analytic approximations to explore it. If it does not appear in the simulation, we will be wary of approximations which give it, carefully looking at the simulation and the approximation to determine what is going on. Next we would like to use simulation to develop a *feeling* for the way in which the physical properties of a model depend upon the parameters in the model. In addition, as noted, simulations can be used to test the utility of various approximate techniques. Finally, one can proceed toward obtaining quantitative numerical results if this is appropriate.

In this overview I plan to focus on the nature of the calculations, reviewing the world-line[3] and exact determinant updating[4] methods we

have used. Illustrations of the way correlations can be studied will be given using the spinless fermion model. The conclusion addresses some additional technical questions that need to be answered in order to fully utilize simulation in the study of quantum condensed matter physics.

2. QUANTUM MONTE CARLO

In classical statistical mechanics the thermal equilibrium average of an observable A is given by

$$\langle A \rangle = \int \prod_i dx_i \, P(x_i) \, A(x_i) \tag{1}$$

with

$$P(x_i) = \frac{e^{-\beta E(x_i)}}{Z} \tag{2}$$

and

$$Z = \int \prod_i dx_i \, e^{-\beta E(x_i)} \tag{3}$$

Metropolis et al.[1] proposed a Monte Carlo method which generated a set of M independent configurations $\{x_i\}_1$, $\{x_i\}_2$,..., $\{x_i\}_M$ distributed according to (2). According to this *importance sampling* algorithm one makes a change in the configuration $\{x_i'\}$ and accepts this new configuration if

$$e^{-\beta E(x_i')} / e^{-\beta E(x_i)} > r \tag{4}$$

where r is a random number distributed between 0 and 1. Typically, local changes are made, $x_i \to x_i + \delta x_i$, and a number of sweeps through the entire lattice $\{x_i\}$ are necessary to make sure that an independent configuration is generated. This algorithm is one of many that satisfies detailed balance and generates configurations distributed according to (2). Once M configurations are generated

$$\langle A \rangle = \frac{1}{M} \sum_{n=1}^{M} A(\{x_i\}_n) \tag{5}$$

with an error which falls as $M^{-1/2}$, provided the system is in equilibrium and the configurations are independent.

For the quantum problem one is interested in calculating

$$\langle A \rangle = \frac{\mathrm{tr}\, e^{-\beta H}}{Z} \tag{6}$$

with

$$Z = \mathrm{tr}\, e^{-\beta H} = \sum_{\alpha} \langle \alpha | e^{-\beta H} | \alpha \rangle \tag{7}$$

Here the sum over $|\alpha\rangle$ represents a sum over a complete set of many-body states. Since H is an operator, we do not in general known how to evaluate $\langle \alpha | e^{-\beta H} | \alpha \rangle$ and cannot proceed as directly as in the classical problem where one has $e^{-\beta E(x_i)}$ with $E(x_i)$ a known c number function of the state $\{x_i\}$. In the quantum problem, one separates $e^{-\beta H}$ into L pieces

$$Z = \sum_{\alpha_1, \alpha_2, \ldots} \langle \alpha_1 | e^{-\Delta\tau H} | \alpha_2 \rangle \langle \alpha_2 | e^{-\Delta\tau H} | \alpha_3 \rangle \cdots \langle \alpha_L | e^{-\Delta\tau H} | \alpha_1 \rangle \tag{8}$$

with $\Delta\tau = \beta/L$. This, in effect, introduces an extra dimension into the quantum problem. Then with $\Delta\tau$ times the characteristic energies in H small one evaluates $\langle \alpha_i | e^{-\Delta\tau H} | \alpha_j \rangle$ by separating H into parts $H_1 + H_2$ which can be individually determined

$$\langle \alpha_i | e^{-\Delta\tau(H_1 + H_2)} | \alpha_j \rangle \simeq \sum_{\alpha_k} \langle \alpha_i | e^{-\Delta\tau H_1} | \alpha_k \rangle \langle \alpha_k | e^{-\Delta\tau H_2} | \alpha_j \rangle + O(\Delta\tau^2) \tag{9}$$

This separation of H can be into kinetic and potential energy pieces or into parts involving separate pieces of the lattice. This latter separation is useful for quantum spin models, many-boson systems, and certain 1-D fermion problems where the matrix elements are positive and can be directly evaluated. However, for fermion problems in higher dimensions, sign problems arising from the Pauli principle lead to severe difficulties with procedures which attempt a direct sum over fermion configurations. In these cases, one integrates out the fermion degrees of freedom leaving a determinantal weight involving a Hubbard–Stratonovich or possibly a phonon field. Here we will illustrate these two techniques in order to see what is involved in carrying out a quantum Monte Carlo simulation.

3. THE WORLD LINE METHOD

Consider a 1-D spinless fermion model

$$H = \sum_{l} -t(c_{l+1}^{+} c_l + c_l^{+} c_{l+1}) + V n_{l+1} n_l \tag{10}$$

For this system, it is convenient to separate H into pieces involving different lattice sites

$$H_1 = \sum_{l(\text{odd})} -t(c_{l+1}^{+} c_l + c_l^{+} c_{l+1}) + V n_{l+1} n_l$$
$$H_2 = \sum_{l(\text{even})} -t(c_{l+1}^{+} c_l + c_l^{+} c_{l+1}) + V n_{l+1} n_l \tag{11}$$

Then, once H_1 and H_2 are separated as shown in (11), the evaluation of $\langle \alpha_i | e^{-\Delta\tau H_1} | \alpha_k \rangle$ and $\langle \alpha_k | e^{-\Delta\tau H_2} | \alpha_j \rangle$ involves only the solution of a two-site problem.

The sum over the set of states $\{\alpha_i\}$ used in calculating Z, (8) and (9) can be viewed as a sum over generalized configurations. Figure 1 shows one such configuration for an eight-site system. Here each state α_i is specified by occupation numbers, and we have connected the occupied sites *world-lines*. The shaded areas correspond to regions in which H_1 or H_2 operate. This checkerboard breakup was used by Barma and Shastry[14] to map 1-D quantum problems onto 2-D classical statistical mechanics problems. In reference 3 we discussed how the checkerboard breakup could be used to cary out Monte Carlo calculations on 1-D fermion systems and quantum spin problems in any dimension. The Monte Carlo procedure parallels the classical method. Starting from an initial configuration $\{\alpha_i\}$, a

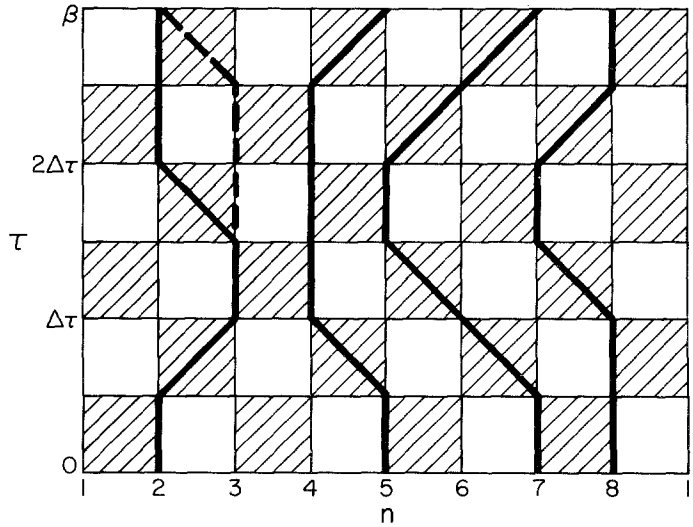

Fig. 1. A quantum field configuration. Fermions can hop and interact in the shaded squares. The dashed line indicates a possible local move generating a new configuration.

change is proposed. This corresponds to moving a world line as shown by the dashed line in Fig. 1. The new configuration $\{\alpha_i'\}$ is kept if

$$\frac{\langle\alpha_1|e^{-\Delta H_1}|\alpha_2'\rangle\langle\alpha_2'|e^{-\Delta\tau H_2}|\alpha_3\rangle}{\langle\alpha_1|e^{-\Delta\tau H_1}|\alpha_2\rangle\langle\alpha_2|e^{\Delta\tau H_2}|\alpha_3\rangle} > r \tag{12}$$

By sweeping through the lattice a suitable number of times, a set of M quantum configurations $\{\alpha_i\}_n$ is obtained. Then

$$\langle A\rangle = \frac{1}{M}\sum_{n=1}^{M} A(\{\alpha_i\}_n) \tag{13}$$

with

$$A(\{\alpha_i\}) = \frac{1}{2L}\sum_{i=1}^{2L}\frac{\langle\alpha_{i+1}|Ae^{-\Delta\tau H_{1,2}}|\alpha_i\rangle}{\langle\alpha_{i+1}|e^{-\Delta\tau H_{1,2}}|\alpha_i\rangle} \tag{14}$$

Here $H_{1,2}$ is H_1 or H_2 depending upon whether i is odd or even.

To see how this works, consider a 40-site half-filled system. Figure 2 shows two typical configurations for $V=0$ and 2.5. Here we have set the hopping $t=1$ so the bandwidth is 4, and taken $\Delta\tau=0.25$. There are 36 times slices corresponding to $\beta=\Delta\tau\cdot 36/2=4.5$ or a ratio of thermal energy

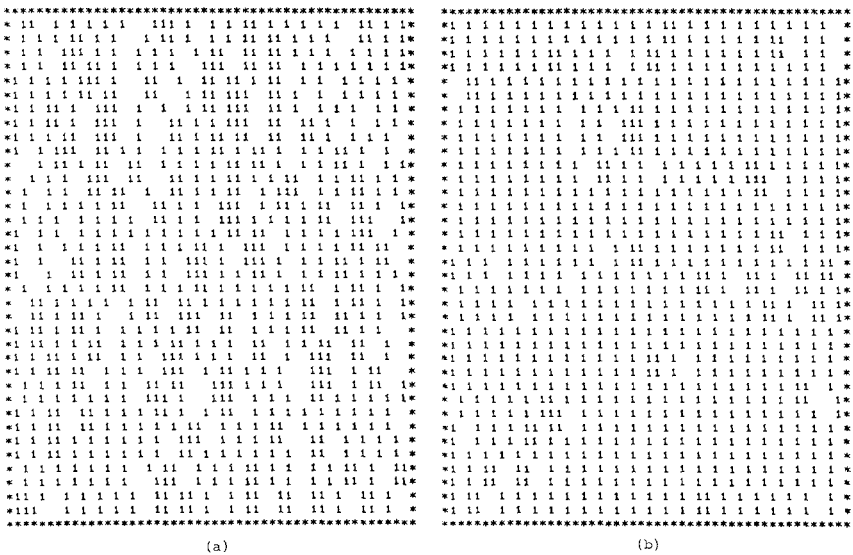

(a) (b)

Fig. 2. Typical configurations for 20 fermions on a 40-site lattice at $\beta=4.5$ for (a) $V=0$ and (b) $V=2.5$.

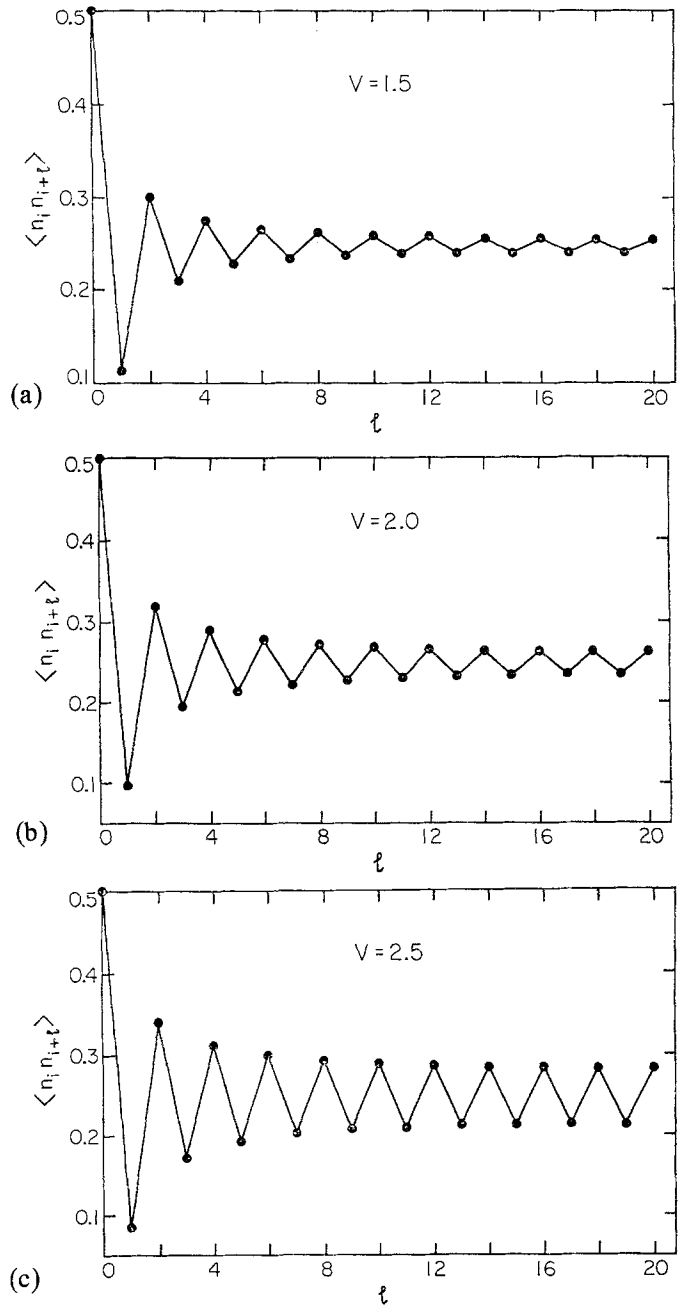

Fig. 3. Equal time density–density correlation functions versus site separation for (a) $V = 1.5$, (b) $V = 2.5$. Here $\beta = 4$.

to bandwidth of $kT/4 = 1/18$. In these figures, a 1 means that a site is occupied, and a blank means that it is empty. Comparing Fig. 2(a) with 2(b), one can clearly see the effect of V in establishing low temperature charge density correlations. A quantitative measure of this can be obtained by calculating the equal time density–density correlation function $\langle n_{i+l} n_i \rangle$, Fig. 3. From the relationship between the spinless fermion model and the Heisenberg XXZ model provided by the Jordan–Wigner transformation, we know that for $V > 2$ there is long-range charge density order in the ground state. Furthermore, for $V < 2$, the charge density correlations decay as $l^{-\eta}$ with $\eta = 1$ at $V = 2$. This type of behavior is clearly seen.

Recently this method has been applied to a 3-D array of chains coupled by interchain Coulomb interactions.[13] Orienting the chains along the x axis, the transverse coupling has the form $V_y n_{\mathbf{i}+\hat{y}} n_{\mathbf{i}} + V_z n_{\mathbf{i}+\hat{z}} n_{\mathbf{i}}$. Note that there is no electron transfer between chains and so there are no fermion sign problems, and the world-line method can be used. The simulation was carried out on a STAR Technologies ST-100 array processor which updated 250,000 sites per second. Figure 4 shows results for the specific heat per site of a 10×10 array of chains, each containing

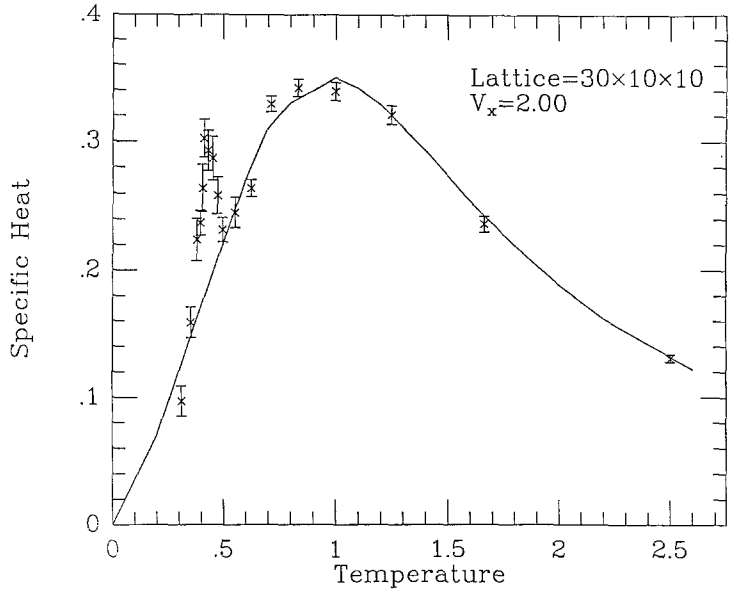

Fig. 4. Specific heat per site versus T for a $30 \times 30 \times 10$ lattice with $V_x = 2$ and $V_y = V_z = 0.2$. The solid curve in the Bonner–Fisher[15] result for a single chain extrapolated from finite chain calculations.

30 sites. Here $V_x = 2$ and $V_y = V_z = 0.2$, corresponding to a quasi-1-D system. The solid line in Fig. 4 represents the Boner–Fisher[15] $N \to \infty$ extrapolation of the specific heat per site for a single chain. As expected, the specific heat of the weakly coupled array initially follows the single chain result until the correlations along the chain become sufficiently long range so that the weak interchain coupling locks the charge density waves on the different chains producing a phase transition at $T = 0.44 \pm 0.02$.

Figure 5 shows the temperature dependence of the structure factor

$$S(\mathbf{q}) = \frac{1}{N} \sum_{l} \sum_{\mathbf{i}} e^{i\mathbf{q} \cdot l} \langle n_{\mathbf{i}+l} n_{\mathbf{i}} \rangle \tag{15}$$

for $\mathbf{q} = (\pi, \pi, \pi)$ and the onset of order at T_c is clearly evident. At higher temperature $S(\mathbf{q})$ first develops a ridge at $q_x = 2p_F = \pi$ and only as T_c is approached does the Bragg peak at $\mathbf{q} = (\pi, \pi, \pi)$ develop. The ridge at $q_x = 2p_F$ corresponds to the diffuse X ray lines observed above T_c in studies of quasi-1-D electron systems. An analysis of the scaling behavior of $S(\pi, \pi, \pi)$ near T_c gives $\gamma = 1.25$ consistent with the expected 3-D Ising behavior. A variety of additional correlations as determined for various coupling parameters, providing detailed information about the development of correlations in quasi-1-D materials. We believe that this work indicates the type of simulations that will ultimately be carried out on interacting fermions with full 3-D motion.

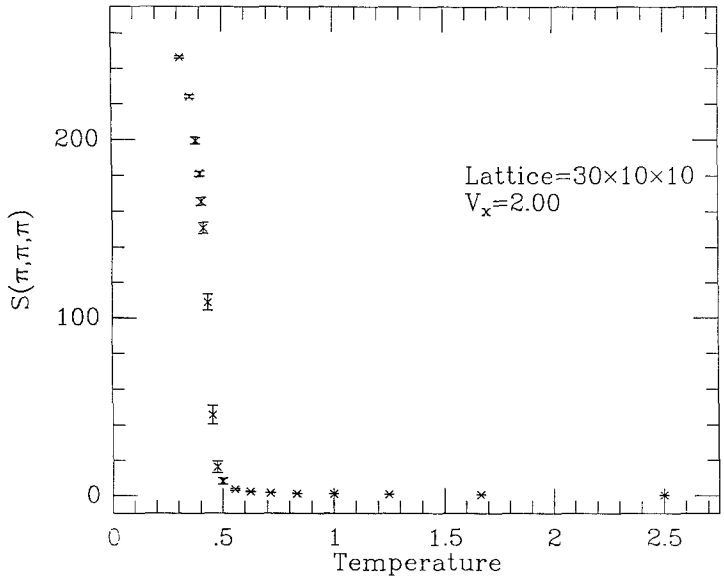

Fig. 5. $S(\pi, \pi, \pi)$ versus T for the same interaction parameters as in Fig. 4.

4. DETERMINANTAL METHOD

When fermions can move around each other, sign problems arise that severely limit simulations which attempt to numerically sum over specific fermion field configurations. In these cases, one can introduce a Hubbard–Stratonovich field to reduce the fermion problem to an effective single particle problem and formally integrate out the fermion degrees of freedom. For fermions, it is possible to use a discrete Hubbard–Stratonovich transformation introduced by Hirsch[16]

$$e^{-\Delta\tau V(n_i-1/2)(n_j-1/2)} = \tfrac{1}{2} e^{-\Delta\tau V/4} \sum_{S_{ij}=\pm 1} e^{-\Delta\tau J S_{ij}(n_i-n_j)} \tag{16}$$

with $\cos h(\Delta\tau J) = e^{\Delta\tau/2}$. In this case, for the spinless fermion model

$$Z = \sum_{\{s_{ij}(\tau_l)=\pm 1\}} \operatorname{tr} e^{-\Delta\tau\tilde{H}(\tau_L)}, \ldots, e^{-\Delta\tau\tilde{H}(\tau_1)} \tag{17}$$

with

$$\begin{aligned}\tilde{H} &= \sum_{(ij)} [-t(c_i^+ c_j + h.c.) + JS_{ij}(\tau)(n_i - n_j)] \\ &\equiv \sum_{(ij)} c_i^+ h_{ij}(\tau) c_j \end{aligned} \tag{18}$$

and the problem is reduced to noninteracting fermions moving in a space-imaginary-time potential $JS_{ij}(\tau)$. Here i and j are near-neighbor sites.

Formally tracing the fermions out

$$Z = \sum_{\{S_{ij}(\tau)\}} \det(1 + B) \tag{19}$$

with $B = B_L \cdots B_1$ and

$$B = e^{-\Delta\tau h(\tau_l)} \tag{20}$$

Here h is the matrix given by (18). In this formulation, a configuration consists of a set of space-time link variables $\{S_{ij}(\tau_l) = \pm 1\}$. In a Monte Carlo (heat-bath) algorithm, a change $\{S\} \to \{S'\}$ [e.g., $S_{23}(\tau_2) \to -S_{23}(\tau_2)$] is proposed and accepted with probability

$$P = 1/(1 + R) \tag{21}$$

where

$$R = \frac{\det[1 + B(S')]}{\det[1 + B(S)]} \tag{22}$$

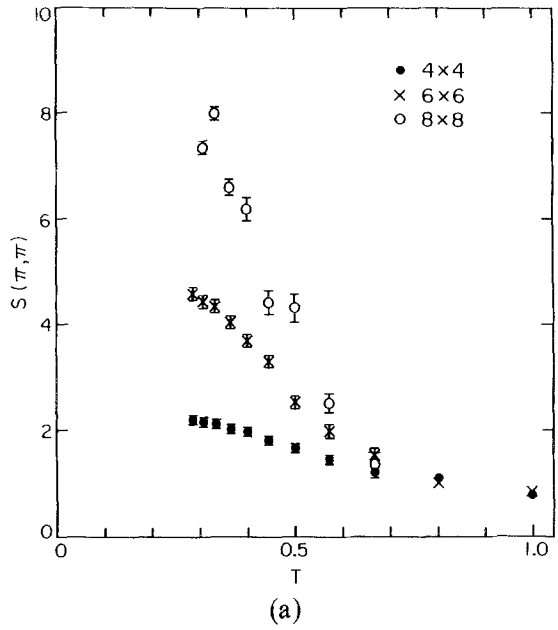

(a)

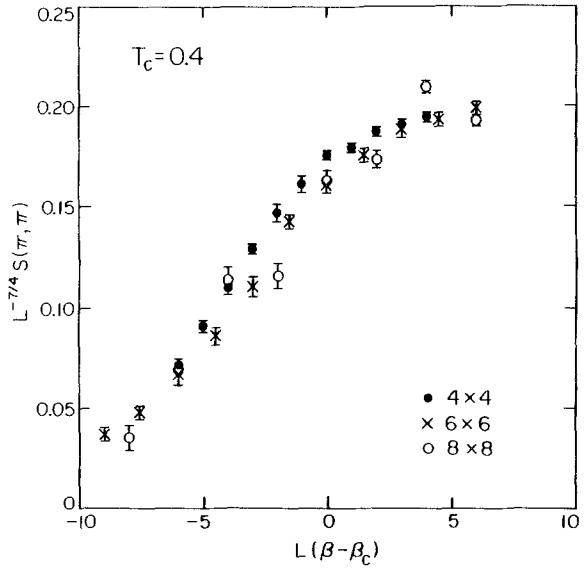

(b)

Fig. 6. (a) The peak in the structure factor $S(\pi, \pi)$ for a 2-D spinless fermion quantum lattice gas versus T for three different lattice sizes: $L = 4$, 6, and 8. Here $V/t = 1$. (b) Scaling plot of the data in (a) using Ising exponents and $T_c = 0.4$.

The difficulty is, of course, the computational time it takes to evaluate this ratio. At present, various simulations have been carried out using an exact updating procedure described in Ref. 4. However, the computation time for this method scales as the square of the number of spatial sites times the total number of space-time sites and hence cannot be used on large 3-D systems. Hirsch[11] has used this approach to study the 2- and 3-D Hubbard model going up to 6^3 sites in 3-D. It has also been used[9] to study the 2-D spinless (or spin-polarized) fermion model on spatial lattices up to 12×12.

The 2-D fermion Hamiltonian

$$H = -t \sum_{ij} (c_i^+ c_j + c_j^+ c_i) + V \sum_{ij} (n_i - \tfrac{1}{2})(n_j - \tfrac{1}{2}) \tag{23}$$

with (ij) near-neighbor pairs represents a quantum generalization of the classical Ising lattice gas. In the strong coupling $V/t \gg 1$ limit, it goes over to the Ising model with an order–disorder phase transition at $\sinh(V/2kT_c) = 1$. In the weak coupling $V/t < 1$ limit, the quantum nature of the system becomes important. As the temperature is lowered, the structure factor $S(q)$ develops a Bragg peak below T_c at $\mathbf{q} = (\pi, \pi)$, which signals the formation of a CDW phase. Figure 6(a) shows $S(\pi, \pi)$ versus T for three different $L \times L$ sized lattices, and Fig. 6(b) shows scaled results. According to finite size scaling, $L^{-7/4} S(\pi, \pi)$ should be a universal function of $L(\beta - \beta_c)$. Here we have used 2-D Ising indices since we are dealing with a scalar-order parameter in 2-D. In this way a critical temperature $T_c = 0.4 \pm 0.05$ was determined. Thus, by making use of finite size techniques it is possible to obtain useful information from lattices which can be simulated in a reasonable time. Naturally, for weak coupling when T_c is small, one needs to go to larger sized lattices, and the simulation becomes more difficult. In this case, it may be possible to use the simulation to obtain information on the short-distance, high-frequency part of the interaction and treat the long wavelength low frequency character analytically.[8] This type of hybrid approach needs further study, as discussed in the conclusion.

5. CONCLUSION

Various stochastic methods for numerically evaluating correlations in interacting many-body systems are available. With the continued advances in algorithms and computers, numerical simulation provides a new tool for both qualitative and quantitative studies. It provides a natural approach to problems in which band structure and particle interactions must be treated

on an equal footing. It has already been used to provide some answers to each of the questions raised in the Introduction. However, rather than review more of what has been done, it seems appropriate to conclude with a partial list of what needs to be done to more fully utilize this new tool.

First, as everyone knows, a more efficient algorithm for treating fermions[3] is needed. We need a method in which the time for a sweep scales as the space-time volume of the lattice. Here various new ideas ranging from pseudo-fermion methods[17] to Langevin techniques[18] are under study.

In addition, one will need to devise efficient renormalization procedures for treating different space-time scales. For eample, in many-electron systems which have second-order charge-density, spin-density, ferromagnetic or pairing transitions one is faced with an instability in the particle-hole or two-particle channel. This instability is a low-frequency, long-wavelength property, and its simulation may well require prohibitively large space-time lattices. However, the effective interaction and the single particle propagator may depend on a range of space-time scales that can be reached with a reasonably sized space-time lattice. This suggests that it would be useful to develop procedures for extracting information on the effective interaction and the single particle self-energy from simulations, and then use these, like Landau parameters, to proceed with analytic calculations of the properties of the particle-hole and particle–particle responses.

We also need more insight into methods for simulating real frequency response properties. When the simulations are carried out in imaginary time, one can of course compute the frequency response at the Matsubara frequencies $i\omega_n$. However, it is extremely delicate to analytically continue numerical data, particularly noisy numerical data. Various methods ranging from Pade extrapolations[19] and positive-definite spectral weight evaluations[20] to a direct simulation procedure[21] have been proposed. However, this remains a difficult and important problem. Finally, there is the problem of interacting quantum systems far from equilibrium. That remains a special challenge.

ACKNOWLEDGMENTS

The work reviewed here has been supported in part by the National Science Foundation under grant no. DMR83-20481 and the Department of Energy under grant no. DE-FG03-85ER45197. The ST-100 Array

[3] One also wants to deal with fermions in an external magnetic field that introduces complex phase factors.

Processor was purchased under NSF-DMR83-20423. We gratefully acknowledge E.I. du Pont de Nemours and Company and the Xerox Corporation for their support.

REFERENCES

1. N. Metropolis, A. Rosenbluth, M. Rosenbluth, A. Teller, and E. Teller, *J. Chem. Phys.* **21**:1087 (1953).
2. M. Susuki, *Commun. Math. Phys.* **51**:183 (1976); M. Suzuki, S. Miyashita, nd A. Kuroda, *Prog. Theor. Phys.* **58**:1377 (1977).
3. J. E. Hirsch, D. J. Scalapino, R. L. Sugar, and R. Blankenbecler, *Phys. Rev. Lett.* **47**:1628 (1981); J. E. Hirsch, R. L. Sugar, D. J. Scalapino, and R. Blankenbecler, *Phys. Rev. B* **26**:5033 (1982).
4. R. Blankenbecler, D. J. Scalapino, and R. L. Sugar, *Phys. Rev. D* **24**:2278 (1981); D. J. Scalapino and R. L. Sugar, *Phys. Rev. B* **24**:4295 (1981).
5. R. Blankenbecler and R. L. Sugar, *Phys. Rev. D* **27**:1304 (1983).
6. J. E. Hirsch and D. J. Scalapino, *Phys. Rev. Lett.* **53**:706 (1984); *Phys. Rev. B* **32**:117 (1985).
7. W. A. Little, *Phys. Rev. A* **134**:1416 (1964).
8. J. E. Hirsch and D. J. Scalapino, to be published.
9. D. J. Scalapino, R. L. Sugar, and W. D. Toussaint, *Phys. Rev. B* **29**:5253 (1984); J. E. Gubernatis, D. J. Scalapino, R. L. Sugar, and W. D. Toussaint, *Phys. Rev. B* **32**:103 (1985).
10. E. Loh, Jr., D. J. Scalapino, and P. M. Grant, *Phys. Rev. B* **31**:4712 (1985); *Physica Scripta* **31**:14 (1985).
11. J. E. Hirsch, *Phys. Rev. Lett.* **51**:1900 (1983).
12. W. Gill and D. J. Scalapino, to be published.
13. D. J. Scalapino, R. L. Sugar, and W. D. Toussaint, to be published.
14. M. Barma and B. S. Shastry, *Phys. Rev. B* **18**:3351 (1978).
15. J. C. Bonner and M. E. Fisher, *Phys. Rev. A* **135**:610 (1964).
16. J. E. Hirsch, *Phys. Rev. B* **28**:4059 (1983).
17. F. Fucito, E. Marinari, G. Parisi, and C. Rebbi, *Nucl. Phys. B* **180**:369 (1981).
18. G. Parisi and Wu Yongshi, *Sci. Sin.* **24**:483 (1981).
19. D. Thirumvalai and B. Berne, *J. Chem. Phys.* **79**:5029 (1983).
20. H. B. Schüttler and D. J. Scalapino, *Phys. Rev.* **55**:1204 (1985).
21. J. E. Hirsch and J. R. Schrieffer, *Phys. Rev. B* **28**:5353 (1983).